Tikrit Journal of Pure Science Vol. 31 (1) 2026

DOI:https://doi.org/10.25130/tjps.v31i1.1918

IRAQI Academic Scientific Journals

Tikrit Journal of Pure Science

ISSN: 1813 – 1662 (Print) --- E-ISSN: 2415 – 1726 (Online)

Journal Homepage: https://tjpsj.org/

Tikrit Journal of Pure Science

Growth and Characterization of Copper Oxide Thin Film for Gas Sensor Application

Noor Lafta Hamadan , Faris Saleh Atallah

Department of Physics, College of Science, University of Tikrit, Tikrit, Iraq

Received: 24 Jan. 2025 **Received in revised forum:** 17 Apr. 2025 **Accepted:** 22 Apr. 2025

Final Proofreading: 15 Jul. 2025 **Available online:** 25 Feb. 2026

ABSTRACT

This study involves the preparation of copper oxide (CuO) thin films on glass substrates for gas-sensing applications via direct current (DC) reactive sputtering. X-ray diffraction (XRD) analysis results indicate that the CuO films possess a polycrystalline structure with a preferred orientation along the (110) direction. The surface roughness was analysed using atomic force microscope (AFM) techniques. The films exhibit roughness values (33.2, 54.85, and 21,44 nm) at the applied voltage (480, 580, and 680 V), respectively. The field-emission scanning electron microscope (FE-SEM) images show CuO nanoparticles with a uniform, homogeneous distribution. The particle sizes of the prepared target nanoparticles start to grow with increasing the applied voltage from (480 – 680 V). The average particle width (diameter) was found to be about (26.25 – 69.1 nm). The optical properties of the prepared copper oxide films in the range (300 – 1100 nm) showed that the optical energy gap decreased gradually from (2.78 – 2.36 eV) with increasing applied voltage from (480 – 680V). CuO thin-film sensors exhibited high sensitivity and responded quickly to nitrogen dioxide (NO_2) and ammonia (NH_3). So, it is observed that exposure of the CuO-based sensor material to a NO2 atmosphere decreases the sensor's resistance, whereas exposure to NH_3 increases it.

Keywords: CuO, Gas sensor, Magnetron sputtering, Structural properties.

Name: Noor Lafta Hamadan **E-mail:** noor.n.hamdan@tu.edu.iq

Tikrit Journal of Pure Science Vol. 31 (1) 2026

DOI:https://doi.org/10.25130/tjps.v31i1.1918

نمو وتوصيف طبقة رقيقة من أكسيد النحاس لتطبيقات استشعار الغاز

نور لفته حمدان، فارس صالح عطاء الله

قسم الفيزياء، كليه العلوم، جامعه تكريت، تكريت، العراق

الملخص

تتضمن هذه الدراسة تحضير أغشية أكسيد النحاس الرقيقة على ركائز زجاجية لاستخدامها كمستشعرات للغاز، باستخدام تقنية الرش المغناطيسي التفاعلي بالتيار المستمر. تظهر الأغشية زيادة في قيم الخشونة مع ارتفاع الجهد المطبق. تشير نتائج تحليل حيود الاشعة السينية (XRD) إلى أن أغشية أكسيد النحاس تمتلك بنية متعددة البلورات مع اتجاه مفضل على طول اتجاه (110). تم تحليل خشونة السطح باستخدام تقنية مجهر القوى الذرية (AFM). تظهر الاغشية قيم خشونة (33.2, 54.85, 21,44 nm) عند جهد المطبق (480, 580, 680 V) على التوالي. توضح صور المجهر الإلكتروني الماسح (FE-SEM) جسيمات أكسيد النحاس النانوية، حيث تعرض الجسيمات بتوزيع موحد ومتجانس. تبدأ أحجام جسيمات الجسيمات النانوية المستهدفة المُحضرة في النمو مع زيادة الجهد المطبق من (480 V) الى (680 V) وُجد أن متوسط عرض الجسيمات (القطر) يتراوح بين (26.25 nm) إلى (69.1 nm) من الخصائص البصرية لأغشية أكسيد النحاس المحضرة ضمن النطاق (300 – 110 nm) وجد أن فجوة الطاقة البصرية للأغشية المحضرة انخفضت تدريجيًا من (2.78 – 2.36 eV) مع زيادة الجهد المطبق من (480 V) الى (680 V). أظهرت مستشعرات الأغشية الرقيقة لأكسيد النحاس حساسية ملحوظة واستجابة سريعة لغازي NO_2و NH_3. لذلك، لوحظ أن تعرض مادة الاستشعار القائمة على أكسيد النحاس لجو غاز NO_2 يقلل من مقاومة المستشعر ويزيدها بوجود NH_3.

INTRODUCTION

Copper oxide thin films were synthesized at room temperature by DC reactive magnetron sputtering, a commonly used physical vapor deposition technique, for NO_2 and NH_3 gas sensing applications[1]. Chemiresistive gas sensors based on metal oxide semiconductors are considered promising tools for detecting low concentrations of toxic, flammable, and explosive gases, owing to their chemical durability, quick response, ease of fabrication, and cost-effectiveness compared to other sensor types[2, 3]. CuO has a variety of physical, structural and optical properties with a band gap energy of (1.21 eV) [4]. It is one of the significant, thermally stable p-type metal oxides preferred for the production of gas sensors (1), and it is a semiconductor that exhibits varying optical behaviour due to stoichiometric deviations arising from its preparation methods and conditions. The direct optical band gap of CuO films has been shown to depend significantly on the fabrication method and the resulting stoichiometric composition[5]. Inhalation of nitrogen dioxide (NO_2), even at low concentrations in the parts-per-million range, poses risks to human health[6]. Creating gas sensors with high sensitivity and selectivity for detecting NO_2 remains essential, though it continues to present technical challenges[7]. Nitrogen dioxide (NO_2) is a reddish-brown oxidizing gas known for its irritating effects. It is commonly produced as a by-product of industrial combustion and vehicle emissions, making it a major air pollutant[8]. Gas sensor sensitivity is the ability to detect gases, or the ratio of the sensing element's resistance in the target gas to that in air. Sensor sensitivity is strongly influenced by factors such as the film's porosity, thickness, operating temperature, and crystallite

DOI:https://doi.org/10.25130/tjps.v31i1.1918

size[9, 10]. This formula was used to determine the gas response. [11]:

$$R_{response}(\%) = \frac{R_{air-Rgas}}{R_{air}} \times 100\% \quad \ldots (1)$$

Where R_{air} is the sensor resistance in air, and Rgas is the sensor resistance in the presence of the gas. The energy gap (Eg) value is calculated by extrapolation of the straight line of the plot of $(\alpha h\nu)^2$ versus photon energy ($h\nu$) for different applied voltages of CuO films. e.g., was calculated by the following relation. [12]:

$$\alpha h\nu = B (h\nu - Eg)^n \quad \ldots (2)$$

where B is a constant, h represents Planck's constant, ν represents the photon frequency, and n represents the type of transition. This work aims to study the structural and physical properties of CuO thin films deposited on glass substrates under various sputtering conditions and to evaluate their use in gas-sensor applications.

1- Experimental Procedure

CuO thin films were fabricated by direct current (DC) reactive magnetron sputtering onto glass substrates. To ensure surface cleanliness, the substrates were initially treated in an argon gas environment to remove impurities and native oxide layers. A turbo molecular pump was utilized to reduce the chamber pressure to approximately 5×10^{-5} mbar. The plasma discharge was established by mixing argon and oxygen gases at an 80:20 ratio using flow meters for each gas source. The sputtering process was conducted at voltages of 480, 580, and 680 V, with a constant pressure of 0.05 mbar and a fixed electrode spacing of 5 cm. Each deposition cycle lasted for 90 minutes.

CuO thin films for gas sensing were prepared by DC reactive sputtering onto glass substrates, and their structural properties were analyzed using XRD, AFM, and FE-SEM, and their optical properties were analyzed using UV-Vis. Gas-sensing measurements were carried out to determine the sensitivity, response time, and recovery time of sputtered CuO thin films. Samples fabricated under optimal sputtering conditions—namely 680 V applied voltage, 0.05 mbar working pressure, and a 5 cm inter-electrode distance—were subjected to gas sensing tests using 20 ppm concentrations of NO_2 and NH_3 at 200 °C. The electrical response was monitored by recording changes in current, reflecting variations in resistivity and conductivity due to gas exposure. The schematic of the sputtering set-up is shown in Figure 1.

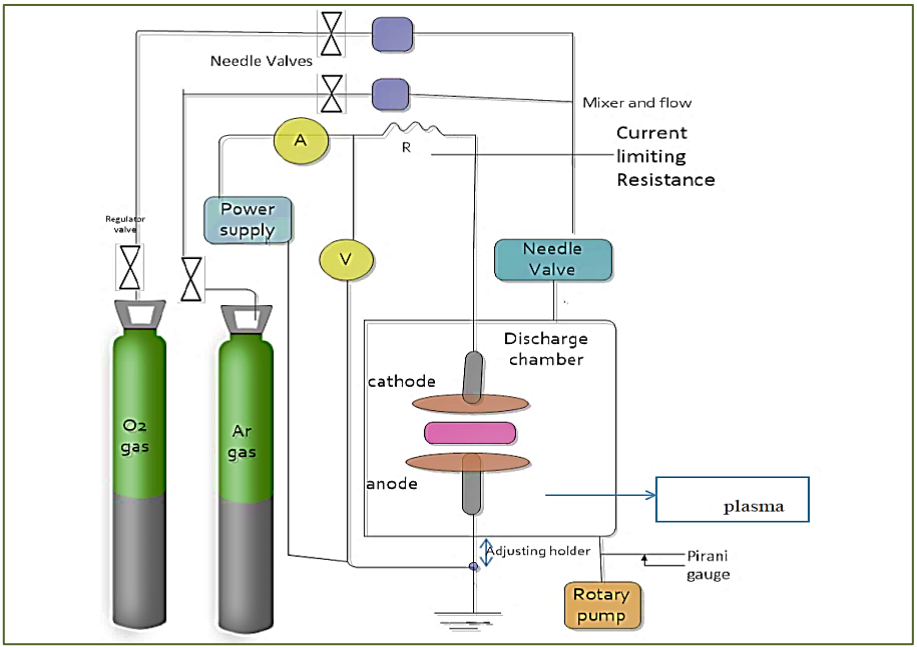

Fig. 1: Schematic of the DC-magnetron sputtering set-up.

DOI:https://doi.org/10.25130/tjps.v31i1.1918

To fabricate the gas sensor, a special mask must be carefully attached to the CuO layer. Aluminum ohmic metal contacts are deposited onto the CuO films by vacuum evaporation. Figure 2 shows the schematic diagram of the electrodes of the CuO gas sensor. The chamber is opened, and the gas sensor is placed on the heater. The necessary electrical connections between the input pin and the sensor were made using a conductive aluminum sheet, and the test chamber is closed. The concentrations of the target gases, NO2 and NH3, inside the chamber were adjusted by monitoring the ratio of the dry air flow rate to the target gas flow rate. The flow rates of the air and the test gas are measured using the needle valves, and the test gas (1, 2, and 3 %) is injected into the air. The resistance of the sensor device was measured using a Keithley 6487 picoammeter/voltage source meter. The gas sensor measurements are performed using a home-designed experimental setup.

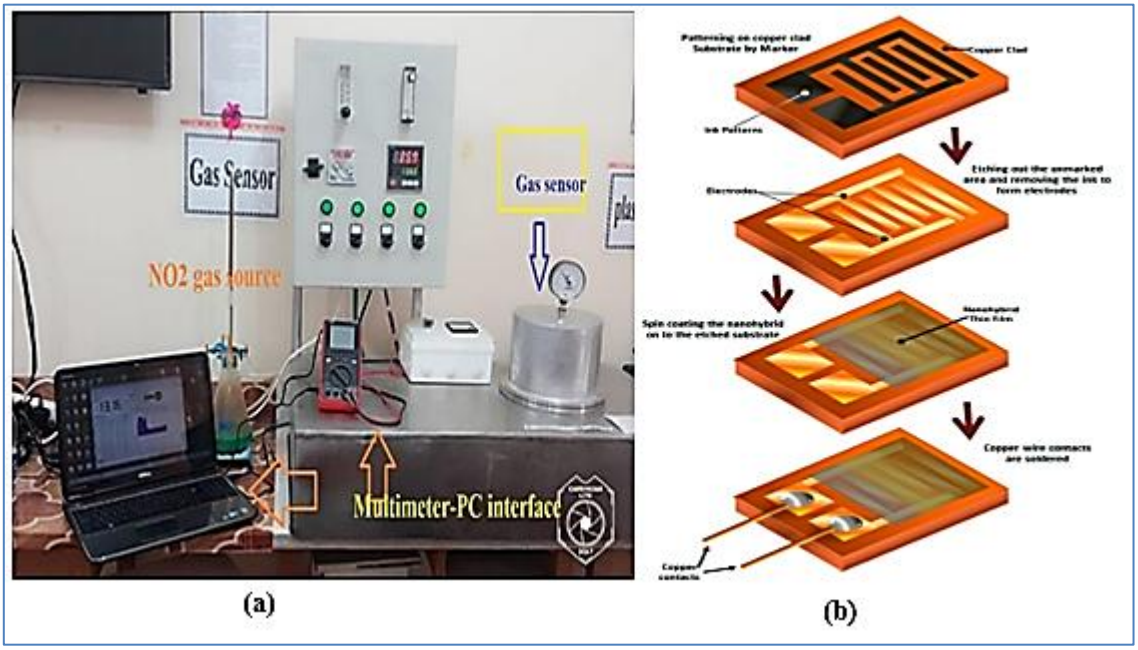

Fig. 2: (a) Gas sensor testing system, (b) Mask used for Gas Sensing.

Results and Discussion

X-ray diffraction (XRD) analysis was employed to assess the crystallinity and estimate the grain size of the CuO thin films deposited at varying voltages. As the applied voltage increased from 480 V to 680 V, the intensity and sharpness of the diffraction peaks also increased, indicating improved crystallinity. The films exhibited multiple orientations, including (110), (111), (-112), (202), (022), and (-222), consistent with the JCPDS card No. 19-901-6106. The increase in peak intensity suggests an increase in crystallite size, as confirmed by Scherrer's equation. [13-15]:

$$D = \frac{K\lambda}{\beta \cos\theta} \quad \ldots (3)$$

Where the wavelength of X-ray is (λ =1.5406 Å), K is a constant, and β is the full width at half maximum (FWHM), which equals (0.94).

DOI:https://doi.org/10.25130/tjps.v31i1.1918

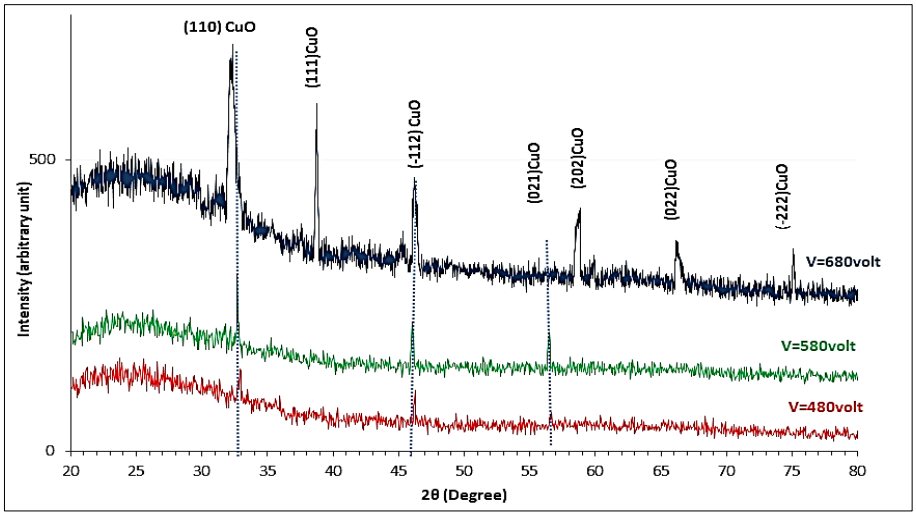

Fig. 3: XRD patterns for CuO thin film deposited at different applied voltages.

Table 1: XRD parameters for CuO thin film deposited by different applied voltages.

Applied voltage (V)	2θ (deg)	FWHM (Deg)	d_{hkl} (Å)	D (nm)	hkl	.Card No	Phase
480	32.95	0.218	2.7522	38	(110)	19-901-6106	CuO (mono)
	46.25	0.3233	1.9632	26.7	(-112)	19-901-6106	CuO (mono)
	56.65	0.205	1.6203	44	(021)	19-901-6106	CuO (mono)
580	32.75	0.218	2.7547	38	(110)	19-901-6327	CuO (mono)
	46.05	0.2322	1.9632	26.7	(-112)	19-901-6327	CuO (mono)
	56.51	0.205	1.6224	44	(021)	19-901-6327	CuO (mono)
680	32.21.93	0.218	2.7639	38	(110)	19-901-6106	CuO (mono)
	38.6938	0.2322	2.3159	26.1	(111)	19-901-6106	CuO (mono)
	46.2203	0.205	1.9557	42.2	(-112)	19-901-6106	CuO (mono)
	58.8253	0.3033	1.5793	30	(202)	19-901-6106	CuO (mono)
	66.1697	0.3433	1.2618	27.6	(022)	19-901-6106	CuO (mono)
	75.09	0.6	1.6233	16.7	(-222)	19-901-6106	CuO (mono)

"The surface topography of CuO thin films, prepared at applied voltages of 480, 580, and 680 V, was analyzed using Atomic Force Microscopy (AFM), as shown in Figures 4 to 6. The results revealed a uniform grain distribution across the film surface, reflecting strong adherence to the substrate. An increase in applied voltage led to the formation of larger grains, thereby increasing surface roughness. This behavior is attributed to the enhanced glow discharge current at higher voltages, which promotes a higher deposition rate of the target material. The granular structure increases surface area, thereby improving gas interaction and enhancing the film's sensitivity. The study confirms that gas sensitivity is positively correlated with surface roughness. [16].

DOI:https://doi.org/10.25130/tjps.v31i1.1918

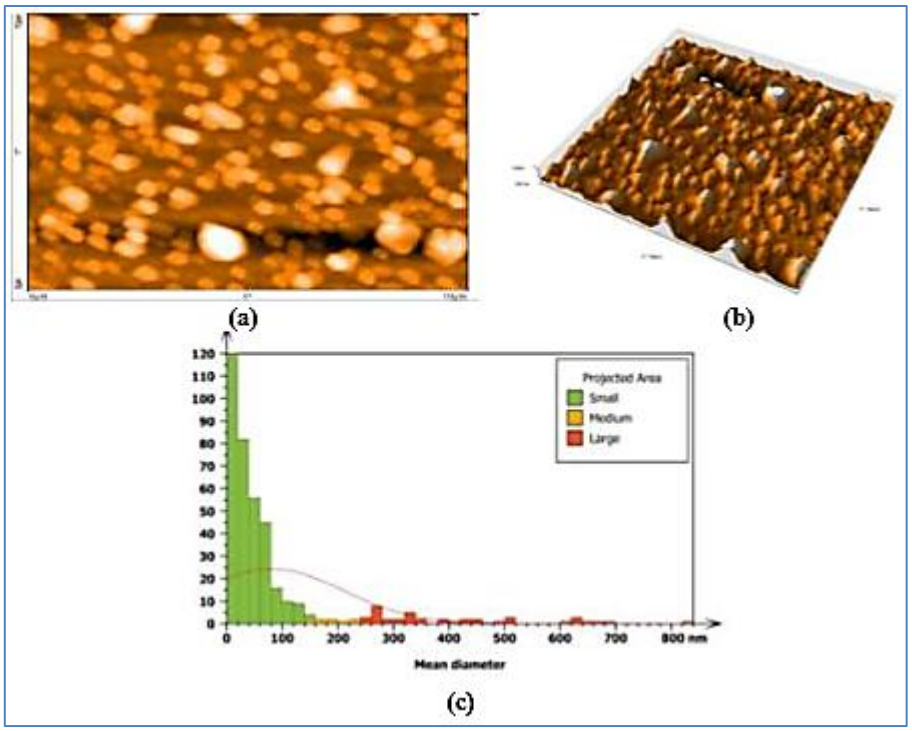

Fig. 4: AFM analysis of CuO thin film deposited on glass substrate by the applied voltage (480 V): (a) two-dimensional image, (b) three-dimensional image, (c) histogram of the grain size distribution.

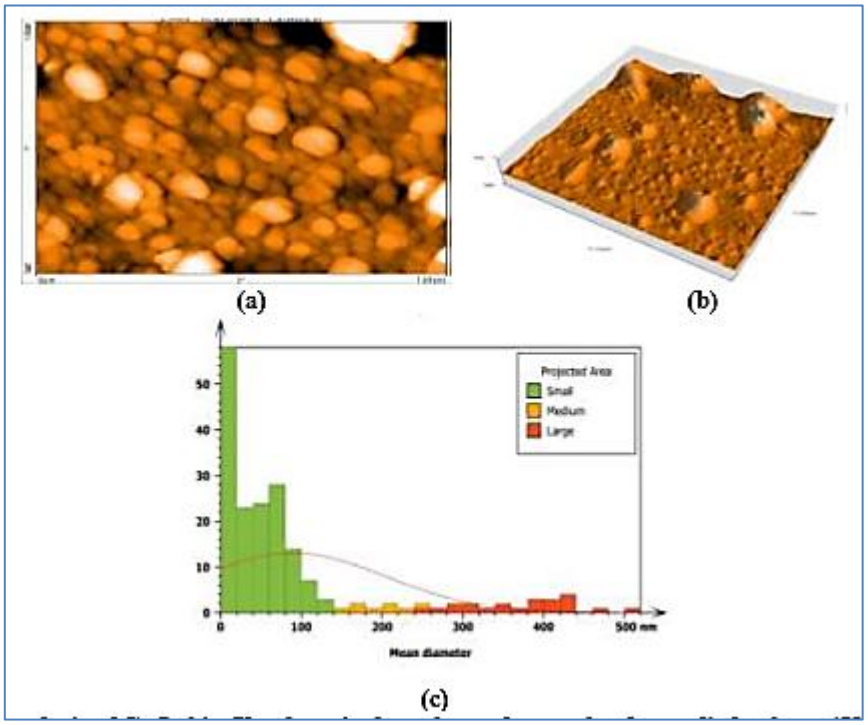

Fig. 5: AFM analysis of CuO thin film deposited on glass substrate by the applied voltage (580 V): (a) two-dimensional image, (b) three-dimensional image, (c) histogram of the grain size distribution.

DOI:https://doi.org/10.25130/tjps.v31i1.1918

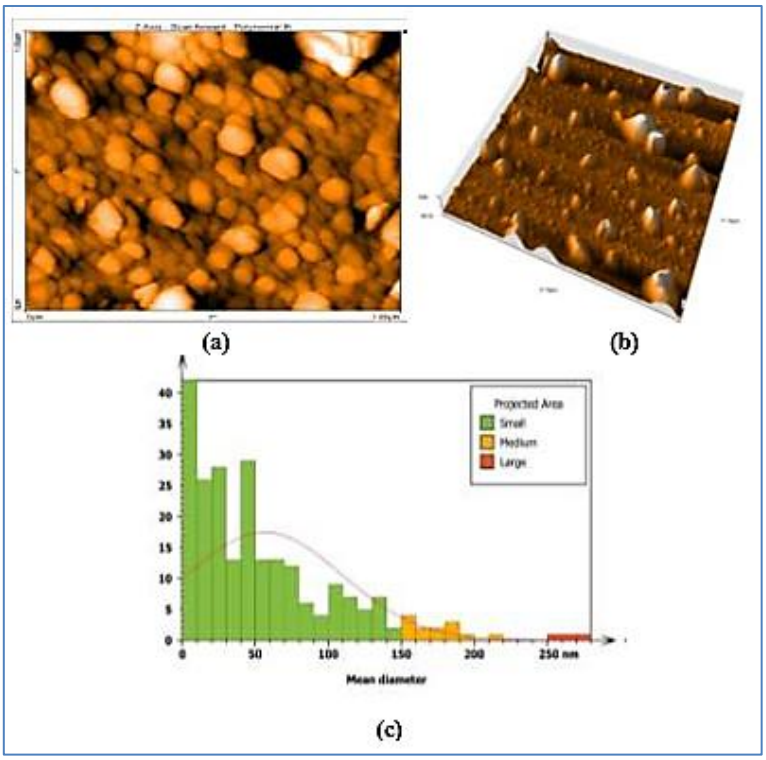

Fig. 6: AFM analysis of CuO thin film deposited on glass substrate by the applied voltage (680 V): (a) two-dimensional image, (b) three-dimensional image, (c) histogram of the grain size distribution.

Field Emission Scanning Electron Microscopy (FE-SEM) was used to study the morphology of CuO thin films deposited on glass substrates under different applied voltages (480, 580, and 680 V), as illustrated in Figures 7 through 9. The micrographs show that the films are composed of nanoscale CuO particles. A clear trend of particle size growth with increasing sputtering voltage is observed, with diameters ranging from approximately 26.25 nm to 69.10 nm. This variation highlights the significant impact of voltage on the nanostructure of the deposited films.

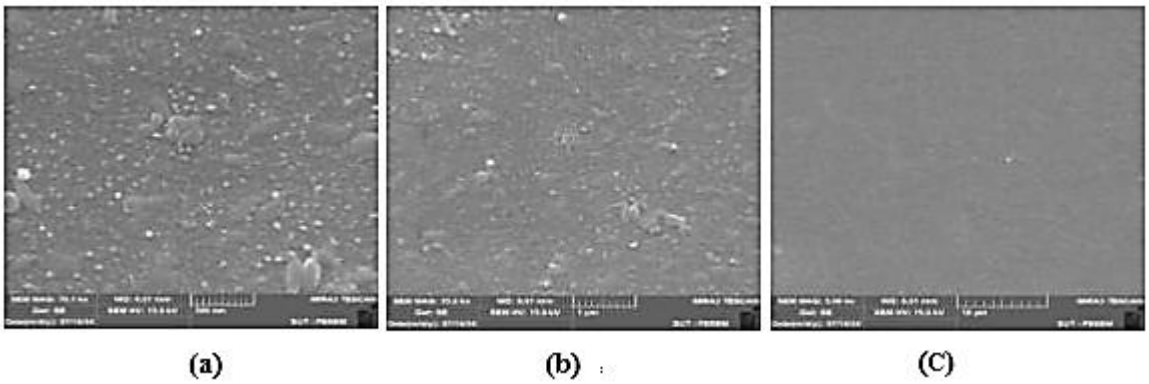

Fig. 7: FE-SEM analysis of CuO thin film deposited on glass substrate by the applied voltage (480 V): (a) at (500 nm) scale, (b) at (1 µm) scale, (c) at (10 µm) scale.

DOI:https://doi.org/10.25130/tjps.v31i1.1918

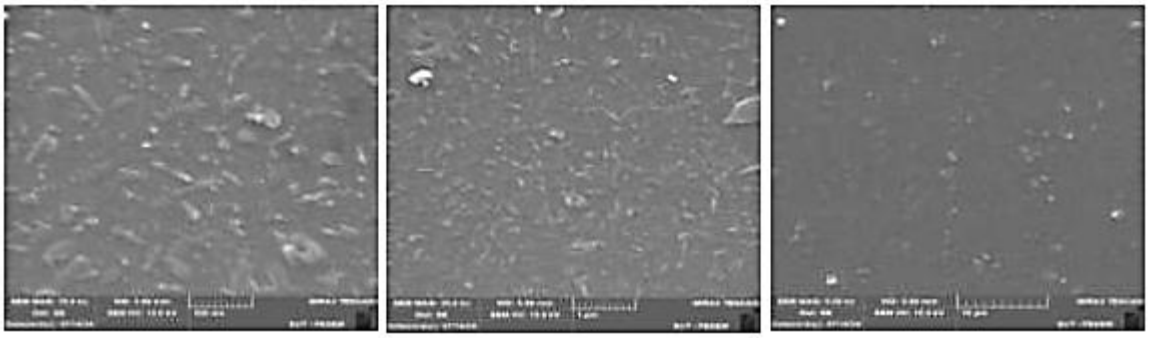

Fig. 8: FE-SEM analysis of CuO thin film deposited on glass substrate by the applied voltage (580 V): (a) at (500 nm) scale, (b) at (1 µm) scale, (c) at (10 µm) scale.

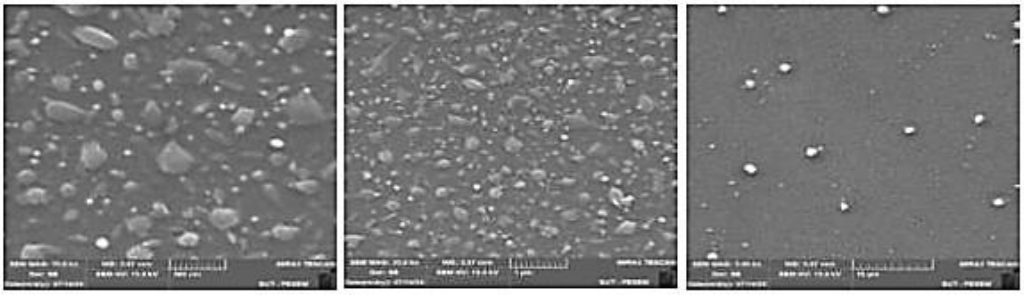

Fig. 9: FE-SEM analysis of CuO thin film deposited on glass substrate by the applied voltage (680 V): (a) at (500 nm) scale, (b) at (1 µm) scale, (c) at (10 µm) scale.

The optical transmission behavior of CuO thin films was examined across a wavelength range of 300 to 1100 nm, as illustrated in Figure 10. A general trend of increasing transmittance with longer wavelengths was observed, demonstrating an inverse relationship with absorbance. The measured transmittance varied with the applied voltage during deposition. Figure 11 shows that all films exhibited high absorbance at lower wavelengths, which decreased gradually as the wavelength increased, particularly in the visible-to-near-infrared range. This phenomenon occurs because, at higher wavelengths, photons possess insufficient energy to interact with the material's atoms and are therefore transmitted. Conversely, shorter wavelengths allow for greater interaction, resulting in higher absorbance. Figure 12 further reveals that the films underwent direct electronic transitions. Additionally, the optical band gap decreased from 2.78 eV to 2.36 eV as the applied voltage increased from 480 V to 680 V, consistent with previously reported findings. [17, 18].

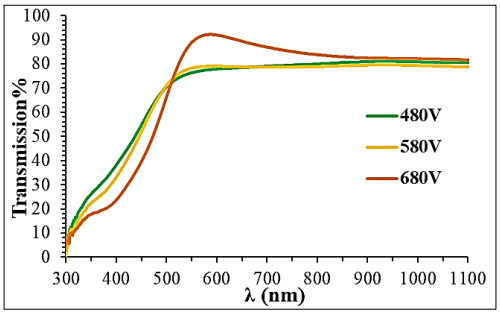

Fig. 10: Transmittance spectrum of CuO thin films at different applied voltages.

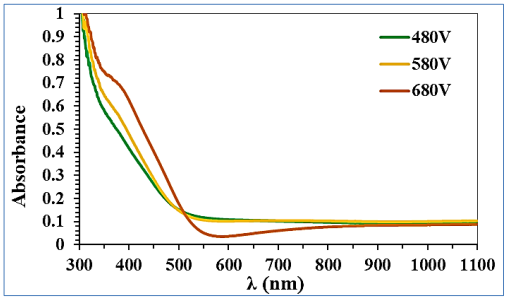

Fig. 11: Absorbance spectrum of CuO thin films at different applied voltages.

DOI:https://doi.org/10.25130/tjps.v31i1.1918

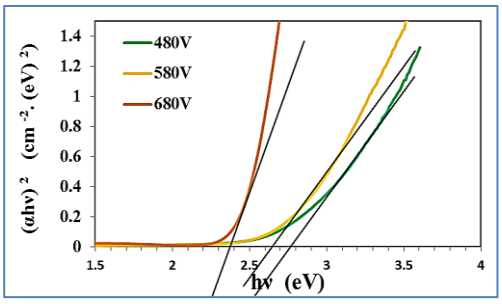

Fig. 12: Energy gap of CuO thin films at different applied voltages.

In this study, the sensing properties of CuO on a glass substrate under optimal operating conditions are investigated as a function of operating temperature and time to determine the temperature dependence of the sensitivity for two different gases, NO_2 and NH_3.

The thin film specimens prepared at applied voltage (680 V), working pressure (0.05 mbar), and inter-electrode spacing (5 cm) were tested for gas sensing using NO2 with a concentration of 20 ppm at an operation temperature of 200 ºC. Figure (13) shows the variation of electrical resistance as a function of time with the on/off gas valve, where the resistance of CuO thin films decreases with time after gas on and increases with time after gas off. This behavior can be attributed to the interaction between the target gas and the metal oxide thin film, typically involving oxygen ions adsorbed on its surface. Such interaction alters the concentration of charge carriers within the material, thereby influencing its electrical conductivity or resistivity. In a p-type semiconductor, where holes are the primary charge carriers, exposure to an oxidizing gas like NO_2 generally leads to an increase in conductivity (or a corresponding drop in resistivity) [19].

DOI:https://doi.org/10.25130/tjps.v31i1.1918

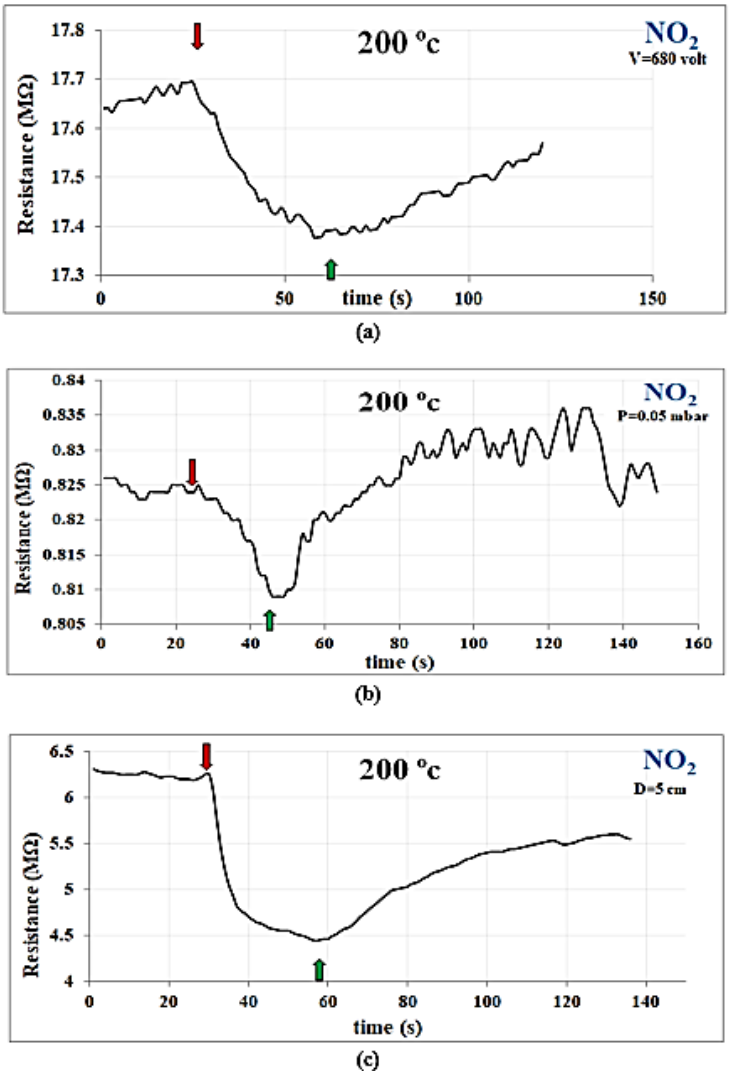

Fig. 13: Resistance response of CuO thin film sensor towards NO_2 gas at the parameters: (a) 680 V, (b) 0.05 mbar, (c) 5 cm.

It is clear from Figure (14) that the resistance of CuO thin films are increase with time after gas on and decrease with time after gas off, the reason for this behavior can be attributed to the that the CuO mechanism sensing associates to the ion sorption of gas type over the surface, leading to charge transfer between the gas and surface molecules and changes in the electrical conductance. Hence, NH_3 is a reducing gas in our environment. When the gas sensor is exposed to ambient reducing gases, the electrons generated by the chemical reaction during the adsorbed oxygen ion-forming process are returned to the conduction band. For the p-type metal oxide semiconductor sensor, the electrons go to the valence band and recombine with the holes, which results in reducing the carrier concentration (holes) and leads to an increase in the sensor resistance and a decrease in electrical conductance[19].

DOI:https://doi.org/10.25130/tjps.v31i1.1918

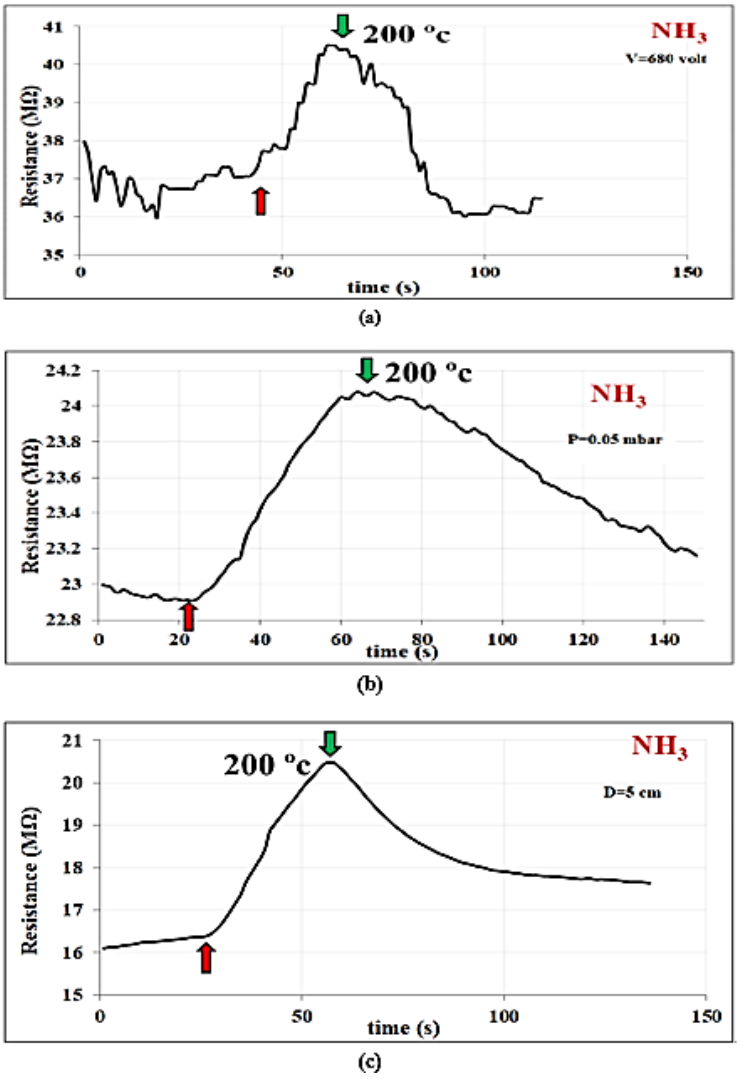

Fig. 14: Resistance response of CuO thin film sensor towards HN_3 gas at the parameters: (a) 680 V, (b) 0.05 mbar, (c) 5 cm.

Table (2) shows the sensitivity for NO_2 prepared and NH_3 gas for CuO samples using the optimal conditions, which include (working pressure 0.05 mbar, applied voltage 680 V and inter-electrode spacing 5 cm). The highest sensitivity of the CuO thin film to NO2 gas is found to be (37.14 %) at an inter-electrode spacing of 5 cm and an operating temperature of 200 °C. The resistance response and recovery time characteristics of the CuO gas sensor exposed to NO2 and NH3 concentrations are shown in Table 2. At the beginning, the measured resistance is steady in air, and then the resistance of the CuO sensor drops in NO2 and recovers to its initial value after NO2 vapor is removed.

Table 2: Gas sensor parameters for CuO thin films using NH_3 and NO_2 gas at optimal working conditions.

Gas sensing (%)	NH_3			NO_2		
	Sensitivity (%)	Response time (s)	Recover time (s)	Sensitivity (%)	Response time (s)	Recover time (s)
Pressure = 0.05mbar	11.11	40	40	1.72	35	70
Distance = 5 cm	26.88	30	40	37.78	27	60
Voltage = 680 V	12.50	37	50	13.64	38	52

DOI:https://doi.org/10.25130/tjps.v31i1.1918

CONCLUSION

From XRD results, it was concluded that the synthesized CuO films have a crystalline structure and exhibit uniform growth of a nanocrystalline film with preferential orientation in the (110) direction. Also, the AFM analysis shows that the CuO images are homogeneous and have a columnar structure. The FE-SEM analysis shows that the deposited coating layer consists of CuO nanoparticles with very small diameters. The particle sizes of the prepared target nanoparticles increase with increasing applied voltage (480-680 V). By recording the transmittance (T) and absorption (A) spectra over the wavelength range, it was found that transmittance increases with increasing applied voltage, while absorption decreases. The energy gap of CuO films was decreased with increased applied voltage. (E_g) values recorded were (2.62, 2.56, and 2.31 eV) at applied voltages of (480, 580, and 680 V), respectively. This section presents the experimental findings on the sensor's responses to NO_2 and NH_3. Their interaction with gas molecules influences the surface morphology of the deposited thin films. The study concluded that the CuO sensor was tested to assess its initial resistance and response behavior upon exposure to NO_2 and NH_3 gases at an operating temperature of 200 °C. The reactions of CuO samples with NO2 and NH3 were observed. The highest sensitivity of the CuO film to NO_2 gas is found to be (37.14 %) and (26.88 %) for NH_3 at (200 °C).

Conflict of interests: The author declared no conflicting interests.

Sources of funding: This research did not receive any specific grant from funding agencies in the public, commercial, or not-for-profit sectors.

Author contributions: The authors contributed equally to the study.

REFERENCES

1. Mahana D, Mauraya AK, Kumaragurubaran S Singh P, Muthusamy SK. Synthesis of CuO thin films by a direct current reactive sputtering process .for CO gas sensing application. Physica Scripta 2023;98(3):035709/https://doi.org .10.1088/1402-4896acb/866

2. Javanmardi S, Nasresfahani S, Sheikhi M. Facile synthesis of PdO/SnO2/CuO nanocomposite with enhanced carbon monoxide gas sensing performance at low operating temperature. Materials research bulletin. 2019;118:110496. https://doi.org/10.1016/j.materresbull.2019.110496

3. Nakate UT, Patil P, Na S-I, Yu Y, Suh E-k, Hahn Y-B. Fabrication and enhanced carbon monoxide gas sensing performance of p-CuO/n-TiO2 heterojunction device. Colloids and Surfaces A: Physicochemical and Engineering Aspects. 2021;612:125962. http://dx.doi.org/10.1016/j.colsurfa.2020.125962

4. Rydosz A, Szkudlarek A. Gas-sensing performance of M-doped CuO-based thin films working at different temperatures upon exposure to propane. Sensors. 2015;15(8):20069-85. https://doi.org/10.3390/s150820069

5. Ogwu A, Bouquerel E, Ademosu O, Moh S, Crossan E, Placido F. An investigation of the surface energy and optical transmittance of copper oxide thin films prepared by reactive magnetron sputtering. Acta Materialia. 2005;53(19):5151-9. https://doi.org/10.1016/j.actamat.2005.07.035

6. Wawrzyniak J. Advancements in improving selectivity of metal oxide semiconductor gas sensors, opening new perspectives for their application in the food industry. Sensors. 2023;23(23):9548. http://dx.doi.org/10.3390/s23239548

7. Ishizuka S, Maruyama T, Akimoto K. Thin-film deposition of Cu2O by reactive radio-frequency magnetron sputtering. Japanese Journal of Applied Physics. 2000;39(8A):L786. http://dx.doi.org/10.1143/JJAP.39.L786

8. Raju P, Li Q. Semiconductor materials and devices for gas sensors. Journal of The .Electrochemical Society2022;169(5):057518 . /https://doi.org10.1149/1945-7111ac/6e0 a

9. Isaac NA, Pikaar I, Biskos G. Metal oxide semiconducting nanomaterials for air quality gas

sensors: operating principles, performance, and synthesis techniques. Microchimica Acta. 2022;189(5):196. https://doi.org/10.1007/s00604-022-05254-0

10.Xie Z, Raju MVR, Stewart AC, Nantz MH, Fu X-A. Imparting sensitivity and selectivity to a gold nanoparticle chemiresistor through thiol monolayer functionalization for sensing acetone. Rsc Advances. 2018;8(62):35618-24. https://doi.org/10.1039/C8RA06137H

11.Rzaij JM. Characterization of CuO thin films for gas sensing applications. Iraqi Journal of Physics. 2016;14(31):1-12. https://doi.org/10.30723/ijp.v14i31.167

12.Khadyair AA, Wanas AH, Zije BA. Study the Structural and Optical Properties of CuO Thin films Prepared by dc Magnetron Sputtering. Journal of Kufa-Physics. 2018;10(2):61-7. https://doi.org/10.31257/2018/JKP/100209

13.Yusuf SI, Mohammad SJ, Ali MH. Study Of The Structural Properties Of Al-Zn Compounds Manufactured By Powder Technology And Copper-Reinforced. Tikrit Journal of Pure Science. 2024;29(2):45-52. https://doi.org/10.25130/tjps.v29i2.1493

14. Abdullah Saeed A. Structural and Optical Properties for ZnO Nanoparticles for Antibacterial .Application. Tikrit Journal of Pure Science 2025;30(1):62-70 . https://doi.org/10.25130/tjps.v30i1.1779

15. Sabah Ahmed B, Jasim Mohammad S, H. Mohammed G. The Effect of Laser Energy on the Structural, Optical and Electrical Properties of CdO Nanomaterials Generated Using (PLD) Technology, and Fabrication of a Gas Sensor. Tikrit Journal of Pure Science. 2024;29(1):107-18. https://doi.org/10.25130/tjps.v29i1.1451

16.Deshpande N, Gudage Y, Sharma R, Vyas J, Kim J, Lee Y. Studies on tin oxide-intercalated polyaniline nanocomposite for ammonia gas sensing applications. Sensors and Actuators B: Chemical. 2009;138(1):76-84. https://doi.org/10.1016/j.snb.2009.02.012

17.Kadhim RG, Ban RSK. Effect of Cd Doping on Structural and Some Optical Studies of Nano CuO Films Prepared by Sol–Gel Technique. World Scientific News. 2017(64):69-83.

18.Hussian SK. Study of the optical properties of Copper Oxide (CuO) thin film prepared by the SPD technique. Al-Muthanna Journal of Pure Science (MJPS). 2017;4(1). https://doi.org/10.18081/2222-4223/017-6/433-152

19.Dhiab S, Hassan NK. Study the Effect of Copper Oxide Nanorods Enhanced by Silver Nanoparticles on the Highly Sensitive Gas Sensor. Tikrit Journal of Pure Science. 2024;29(2):67-73. https://doi.org/10.25130/tjps.v29i2.1521